

Bending instability in galaxies: the stellar disk thickness and the mass of spheroidal component

N.V. Tyurina¹

tiurina@sai.msu.ru

A.V. Khoperskov²

khopersk@sai.msu.ru

and

D. Bizyaev^{1,3}

dmbiz@sai.msu.ru

May 06, 2004

ABSTRACT

We present results of numerical N-body simulations of a galactic stellar disk embedded into a spherical dark halo. The non-linear dynamics of bending instabilities developing in the disk is studied. The bending modes, axisymmetric and not, are considered as main factors increasing the disk thickness. The relation between the disk vertical scale height and the halo+bulge-to-disk mass ratio is inferred. The method of estimation of the spherical-to-disk mass ratio for edge-on spiral galaxies based on this relation is studied and applied to constrain the spherical subsystem mass and the mass of dark halos (M_h/M_d) in seven edge-on galaxies. The values of M_h/M_d are of order 1 for our galaxies.

Subject headings: edge-on galaxies, bending instability, halo, N-body simulations, galactic structure

¹Sternberg Astronomical Institute, Moscow, 119899, Russia

²Volgograd State University, Volgograd, 400062, Russia

³Physics Department, University of Texas at El Paso, TX, USA

1. Introduction

The luminous matter represents only a part of overall mass in galaxies. One of arguments for massive dark matter component comes from numerical simulations of galaxies. Thus, numerical models evaluated for disk galaxies with light spheroidal subsystem show that their stellar disks heat themselves significantly during the evolution achieving the equilibrium state with too high velocity dispersion (Ostriker & Peebles 1973; Carlberg & Sellwood 1985; Athanasoula & Sellwood 1986; Bottema & Gerritsen 1997; Fuchs & von Linden 1998), (Khoperskov et al. 2003). To explain the low ratio of velocity dispersion to the gas rotational velocity c^{obs}/V_c in outer parts which is often observed in many galaxies, one should consider a spherical subsystem as massive as the galactic disk in its optical limits.

The vertical scale height of stellar disk depends on the local disk surface density and the spheroidal subsystem mass M_s . Then, for the case of edge-on galaxies we are enabled to include the observed disk thickness into the numerical simulations. The disk thickness is available from observations for many edge-on spiral galaxies. On the other hand, if the velocity dispersion is close to the required for the marginal stability of the stellar disk, its thickness is tied up with the mass ratio of disk to the spherical component (Zasov et al. 1991; Mikhailova et al. 2001).

An important mechanism of the vertical velocity dispersion c_z growth is the bending instability. The bending instability in galactic disks has been considered with the help of N-body simulations. Important results were obtained when the tidal interactions were taken into account (Hernquist et al. 1993; Weinberg 1998; Velazquez & White 1999; Mayer et al. 2001; Bailin & Steinmetz 2003; Reshetnikov & Combes 2002). The conditions for emerging the bending instabilities were investigated by (Raha et al. 1991; Sellwood 1996; Sellwood & Merritt 1994; Patsis et al. 2002; Griv et al. 2002; Binney et al. 1998), (Sotnikova & Rodionov 2003).

In this paper we point our attention to the radial distribution of c_z/c_r and to the thickness of the stellar disk needed to provide its stability against different kinds of bending perturbations. We consider the late type galaxies without a prominent bulge because the rotation curve in very central regions is not surely defined. The presence of bulge would complicate the analysis of bending instability. The bulge plays a stabilizing role for bending instability when all other conditions being similar. If no bulge presents, one can restore the internal part of rotation curve assuming it is defined by the disk component in central ($r \lesssim 2L$) regions (1). Here L denotes the exponential scale length of the stellar disk.

We performed numerical N-body simulations for seven edge-on galaxies with known photometric scales, both radial and vertical.

Our basic interest throughout the paper is to follow up the evolution of the disk thickness and the behaviour of c_z/c_r ratio that holds the stellar disk in stability against the bending perturbations.

2. Dynamical modeling of edge-on galaxies

We evaluated free parameters of the model: $\mu = M_s/M_d$, the radial scale of the halo a_h , and the disk central surface density σ_0 , looking for the optimal agreement between the calculated and observed values of the disk thickness. Here M_d is the galactic disk mass, $M_s = M_h + M_b$ is the mass of the spherical component which comprises of halo and bulge in general case. Note that since almost all our galaxies have no visible bulge, their spherical component means the galactic dark halo.

Our dynamical modeling is based on the numerical integration of the motion equations for N gravitationally interacting particles. This system of collisionless particles forms a disk embedded into dark halo and bulge. The steady state distribution of mass in the bulge $\varrho^{(b)}$ and halo $\varrho^{(h)}$ is defined as:

$$\varrho^{(h,b)}(\xi) = \frac{\varrho_0^{(h,b)}}{(1 + \xi^2/a_{(h,b)}^2)^k}, \quad (1)$$

where $\xi = \sqrt{r^2 + z^2}$, and r, z are the radial and vertical coordinates, k equals to 3/2 for the bulge and to 1 for the halo. The dimensional spatial scales for the bulge and halo are denoted as a_b and a_h , respectively. We supposed that the bulge is encompassed by a sphere with radius of $\xi \leq r_b^{\max}$.

The initial vertical equilibrium of the disk is defined by the Poisson equation

$$\frac{\partial}{r\partial r} \left(r \frac{\partial \Phi}{\partial r} \right) + \frac{\partial^2 \Phi}{\partial z^2} = 4\pi G (\varrho + \varrho^h + \varrho^b) \quad (2)$$

and by balance of forces in the vertical direction in first approximation

$$c_z^2 \frac{\partial \varrho}{\partial z} = -\varrho \frac{\partial \Phi}{\partial z}. \quad (3)$$

Here Φ is the gravitational potential, ϱ is the disk volume density, and c_z is the vertical component of velocity dispersion. The radial component of the Jeans equation defines the rotation velocity in the stellar disk (Valluri 1994):

$$V^2 = V_c^2 + c_r^2 \left\{ 1 - \frac{c_\varphi^2}{c_r^2} + \frac{r}{\varrho c_r^2} \frac{\partial(\varrho c_r^2)}{\partial r} + \frac{r}{c_r^2} \frac{\partial \langle uw \rangle}{\partial z} \right\}, \quad (4)$$

The last term in the figured brackets in (4) is the chaotic part of the radial u and vertical w velocity components. We distinguish between the circular velocity $V_c = \sqrt{r(\partial\Phi/\partial r)|_{z=0}}$ and the stellar rotation curve $V(r) = r\Omega$ because of the velocity dispersion.

The system of equations (2)–(3) can be reduced to the equation for the dimensionless disk density $f(z; r) = \varrho(z; r)/\varrho(z = 0; r)$ (Bahcall 1984):

$$\frac{d^2 f}{dz^2} + 2 \frac{d \ln c_z}{dz} \frac{df}{dz} - \frac{1}{f} \left(\frac{df}{dz} \right)^2 + \frac{4\pi G}{c_z^2} \frac{\sigma}{2z_0} f \left(f + \frac{2\varrho_h^{eff}}{\sigma} z_0 \right) = 0. \quad (5)$$

where the surface density is equal to $\sigma = 2\varrho(z = 0) \cdot z_0$, $\varrho_h^{eff} = \varrho_h - \frac{1}{4\pi G r} \frac{\partial V_c^2}{\partial r}$, and the vertical scale of the disk is defined as $z_0 = \int_0^\infty f dz$. The circular velocity is defined in the galactic plane $z = 0$. For the case of $c_z = \text{const}$ and $\varrho_h^{eff} = 0$, the disk volume density profile in the vertical direction is:

$$\varrho(z) = \varrho(z = 0) \cdot \text{sech}^2(z/z_0), \quad (6)$$

where we designated the vertical disk scale as $z_0 = c_z^2/\pi G\sigma$. We suppose that the density distribution in a galaxy follows the brightness distribution. It corresponds to the constancy of the mass-to-luminosity ratio. We consider two possible laws for the vertical density distribution $\varrho(z)$: $\exp(-z/h_z)$ and $\text{sech}^2(z/z_0)$. The values of h_z and z_0 are computed as functions of time and location in disk. The radial density profile in the disk is assumed to be exponential $\varrho(r) = \exp(-r/L)$. The mass of the dark halo M_h is calculated inside the maximum disk radius R_{max} . As a rule, $R_{\text{max}} \approx 4L$ (van der Kruit & Searle 1981; van der Kruit & Searle 1982; Pohlen et al. 2002; Holley-Bockelmann & Mihos 2001).

We assume this kind of axisymmetric models in the equilibrium state as initial templates for our simulations. The initial radial distributions of the radial (c_r) and azimuthal ($c_\varphi = c_r \alpha/2\Omega$) velocity dispersions keeps the disk in gravitationally stable state.

Considering edge-on galaxies, we encounter a well known problem that their observed structural parameters are averaged along the line of sight. Once we compare the model parameters with observations, this effect has to be taken into account when we reproduce the model rotation curves as well as the radial and vertical photometric profiles. Deriving

the surface density, we integrated the volume density of the model disk along the line of sight. The same integration was performed for the rotation curves as well, see also (1).

3. The bending instabilities in stellar disks

The disk scale height depends on the vertical velocity dispersion $c_z(r)$, and the latter is dependent of the radial velocity dispersion $c_r(r)$. A discussion about the relation between c_r and c_z was opened firstly by Toomre (Toomre 1966). Considering a simplified model of an infinitely thin uniform self-gravitating layer, (Poliachenko & Shuhman 1977) found that an essential condition for the system stability against the small-scale bending perturbations is $c_z/c_r \geq 0.37$.

The dynamics of the bending instabilities taking a nonuniform volume density distribution in z -direction into account was also considered by (Araki 1986) where a lower value of the critical ratio $c_z/c_r \gtrsim 0.3$ was inferred, see also discussion in (Merrit & Sellwood 1994). The linear analysis of stability against global bending perturbations was discussed by (Poliachenko & Shuhman 1979) and generalized by (Vandervoort 1991).

3.1. The bending instability

Let's consider the dynamics of global bending perturbations. The stellar disks at the initial moment ($t = 0$) were: 1) axisymmetric, 2) in an equilibrium state along the radial and vertical directions, 3) gravitationally stable in the disk's plane (it was made by assuming a high value for the radial velocity dispersion $c_r \gtrsim (1.5 \div 4) \cdot c_T$, the ratio $Q_T = c_r/c_T$ is a function of r (Khoperskov et al. 2003). The disks could be either stable or unstable against the bending perturbations in dependence of $c_z(r)$ distribution. The scale height z_0 and velocity dispersion depend of each other (Bahcall 1984), hence lesser value of c_z corresponds to a thinner disk.

The evolution of systems with a small initial value of c_z/c_r (i.e. the system that is dynamically cold in the vertical direction) reveals a gradual growth of the global bending instability which heats the disk up in the vertical direction, and rises its thickness.

The bending mode $m = 0$. The developing of unstable axisymmetric bending mode ($m = 0$) leads to the significant disk heating in the vertical direction (Sellwood 1996). Let's consider the stellar disk where the axisymmetric mode is developing. The evolution of the vertical coordinate of the disk's local barycenter $\zeta(r, t)$, the vertical velocity dispersion $c_z(r, t)$, the disk scale height $z_0(r, t)$, the dispersion ratio $\alpha_z \equiv c_z(r, t)/c_r(r, t)$, the radial

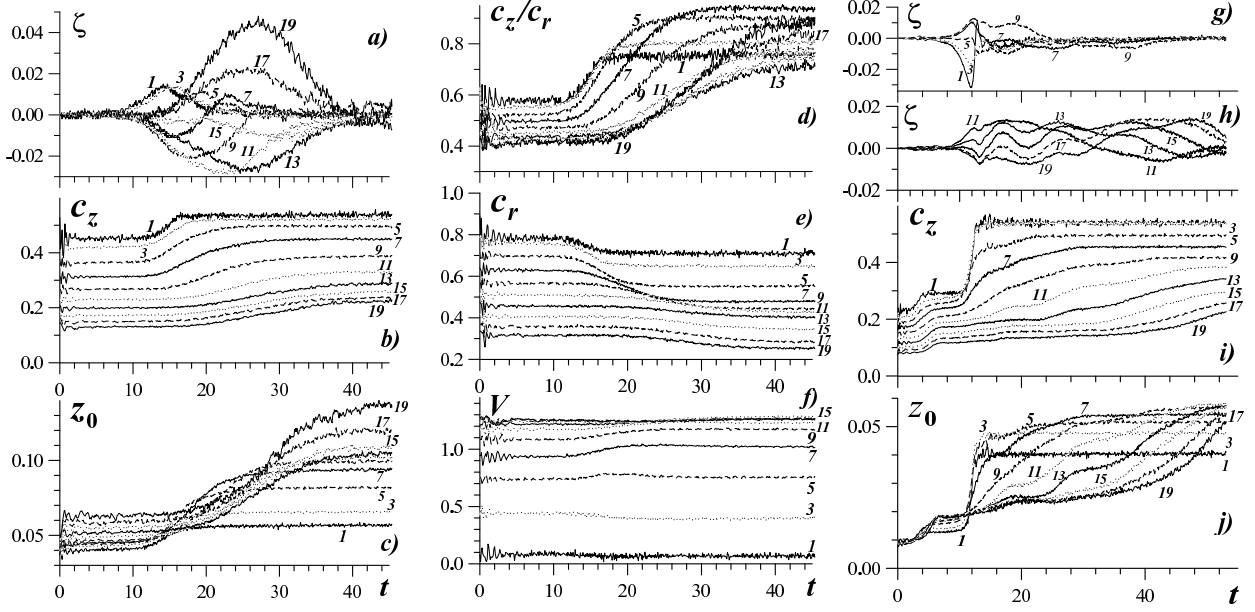


Fig. 1.— Evolution of the stellar disk parameters when the axisymmetric bending mode being developed in the model with $\mu = 1$, $a = L$: a) the vertical coordinate of the disk’s local barycenter ζ , b) vertical component of the velocity dispersion c_z , c) disk’s scale height z_0 , d) the vertical to radial velocity dispersion ratio c_z/c_r , e) c_r , f) rotational velocity of particles in the disk V . g) — i) The same for the model with $\mu = 4$. The vertical coordinate of barycenter ζ for the internal and external regions is shown in separated plots g) and h) respectively. Different curves are drawn for a set of distances to the center $r_j = 4L \cdot (0.05j - 0.025)$, where j is shown in the plots. All the parameters are averaged by the azimuthal coordinate.

velocity dispersion $c_r(r, t)$, and the rotational velocity $V(r, t)$ is shown in Fig.1. We fix the units by the assumption $M_d = 1$, $G = 1$, $4L = 1$.

As it is seen in Fig.1, the parameters of the disk stay unchanged for the first 2.5 turns ($t \approx 10$ in our units). This time the modes are formed at the linear stage of the bending instability evolution. After $t \gtrsim 10$ it changes to the nonlinear development of the bending instability and the barycenter $\zeta(r)$ oscillates with larger amplitude in z -direction (see Fig.1a). In the central regions of the disk the amplitude $\zeta(r)$ rises up faster to its maximum value and falls then down to the initial value (see curves 1-5 in Fig.1a), whereas the growth of $\zeta(r)$ occurs much slower at the outer parts of the disk (curves 11-19). The rapid growth of the velocity dispersion c_z and of the vertical scale height z_0 begins after a time delay from $\zeta(r)$, see Fig.1b and 1c. The flare emerges in the disk’s central region and then propagates toward its periphery. The value of c_z/c_r rises up mostly because of c_z growth, and due to c_r decrease as well (Fig.1 d, e). The azimuthal component of velocity dispersion c_φ follows c_r and the

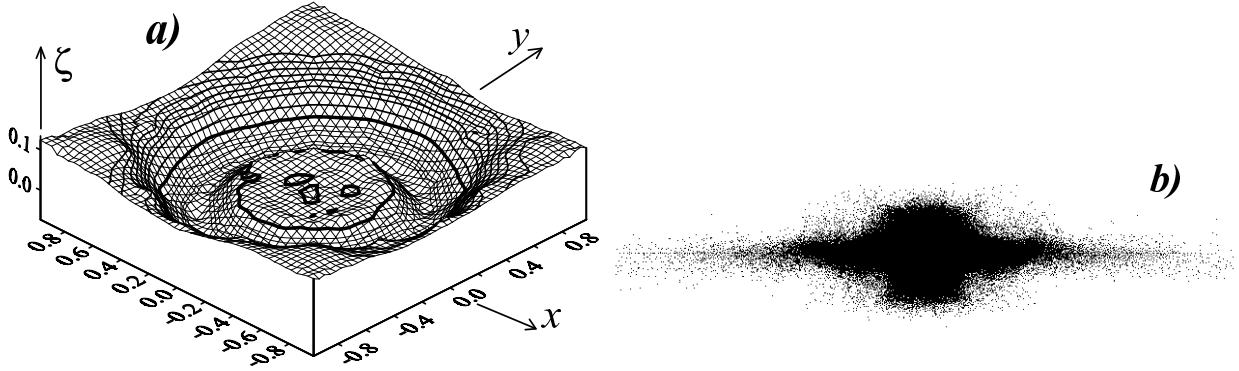


Fig. 2.— The shape of the stellar disk under the development of the bending instability at the moment $t = 25.4$ for the model shown in Fig.1 a–f. Distribution of the vertical coordinate of the barycenter $\zeta(x, y)$ are shown in the $x - y$ plane (a). The bold solid line represents $\zeta = 0$. b) The edge-on view to the disk on the stage of the global axisymmetric mode development. The vertical/plane aspect ratio is increased 4 times.

relation $c_\varphi \simeq c_r \alpha / 2\Omega$ is valid almost everywhere. The equation can be failed only either in a very thick disk or in regions where $z_0/L \gtrsim 0.4$. Note that $c_r/c_\varphi < 2\Omega/\alpha$ that means the anisotropy is lesser in those regions because of the system spherization. The decrease of c_r and c_φ is a result of conversion of the kinetic energy of random motion in the disk plane to the kinetic energy of vertical motions. Note that the development of this bending mode takes place in the disk which is axisymmetric in all parameters.

The value of ζ has different signs in disk’s center and periphery (see Fig.1a), what causes a “mexican hat-like” structure formation as a result of this instability (Fig.2). The isolines of ζ have a concentric shape. Up to the moment $t = 25.4 = 6\tau$ the internal ring and the periphery are shifted off the disk plane toward opposite directions, whereas the central region ($r \lesssim 0.4$) has returned to its initial state. The disk vertical structure driven by the bending mode $m = 0$ is shown in Fig.2b. One can see a box-like shape of the disk which is typical for all models where the axisymmetric bending mode dominates and this feature is not relevant to a bar.

A gradual change of the velocity dispersion c_z and c_r , and rotational velocity V begins when the amplitude of the vertical oscillations ζ grows significantly. The vertical disk heating is accompanied by increase of c_z/c_r but starting with certain values of c_z/c_r the favourable conditions for developing of the bending instability disappear. As a result, new stable and thick disk forms. The characteristic time for this process depends significantly on the model parameters and is of order ten turns of the disks’ outer regions. If the initial distribution of $\alpha_z = c_z/c_r$ is subcritical, the linear stage may take longer time due to low increment

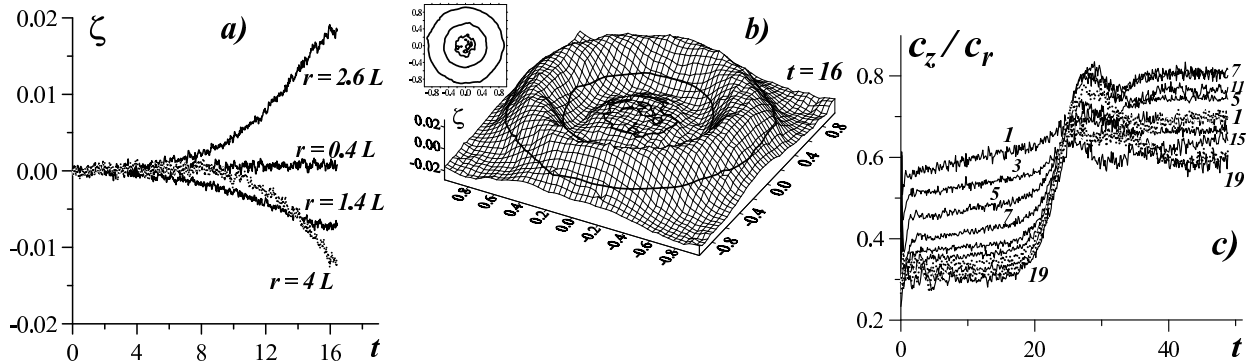


Fig. 3.— The model with $\mu = 4$. a) Initial moments of the vertical displacement evolution at different distances from the center of the disk. b) The shape of the stellar disk (i.e. distribution of z -coordinate of its local barycenter through the disk). The thick line corresponds to $\zeta = 0$. c) The flare of the disk without a halo but in presence of a bulge ($M_b = 0.25 M_d$, $b = 0.2 L$) after the development of the mode $m = 0$. In the regions of bulge the disk thickening is not significant. The notation is kept the same as in Fig.1.

of instability, and heating at the nonlinear stage appears feeble. Hence, the amplitude of the bending mode and even the ability of its emerging mostly depend on the initial radial distribution of c_z/c_r .

The important consequence is that the final distribution of $\alpha_z(r)$, as a result of bending perturbations, depends on its initial value $\alpha_z(r, t = 0)$. Thin disks which have a low value of the scale height after the action of the global bending instability get the larger ratio c_z/c_r than it would required to keep the disk stable. The explanation lays in the essentially nonlinear nature of the disk heating. The parameter c_z/c_r passes through the “zone of stability” and stays off it and c_z/c_r jumps over its marginal threshold.

If the disk is hot enough to provide the gravitational stability against the bar mode and the mass of halo is low ($\mu \lesssim 1$), the main cause of heating the previously thin cold disk is the axisymmetric bending mode ($m=0$) whereas the modes $m=1,2$ do not emerge at all. Note that the mode $m=0$ might start forming far from the center ($r \gtrsim L$) not penetrating into the central part of disk. It can happen by two ways: 1) the initial disk has $c_z/c_r \geq \alpha_z^{crit}$ and is stable in the central regions whereas the periphery of the disk is thin and unstable (Fig.3 a, b); 2) when the galaxy has a concentrated and massive bulge (Fig.3 c). In such models the bending modes in the center have lesser amplitude and, in general, a bulge, as well as a halo, plays a stabilizing role. Hence, having all other equal conditions, the disks of galaxies owing bulges are thinner. Note that we don’t consider dynamical models for the

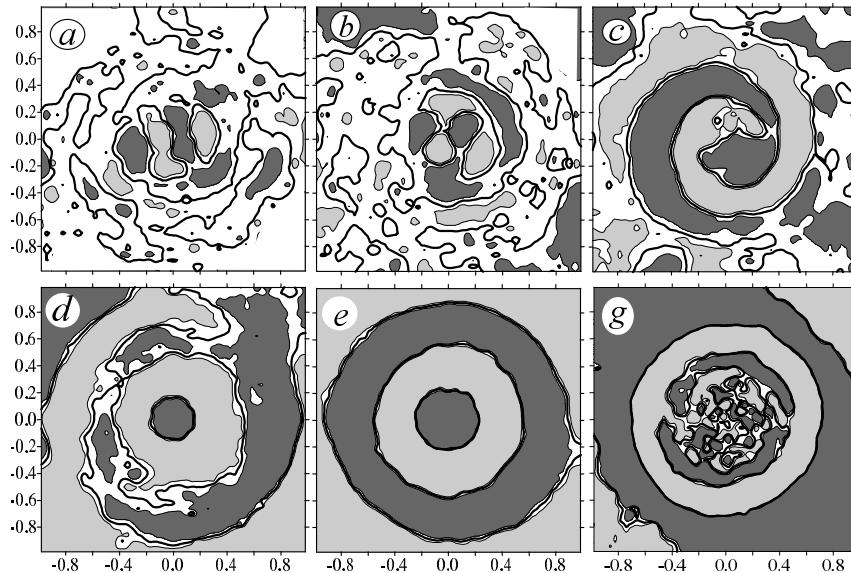


Fig. 4.— The structure of the vertical displacement $\zeta(x, y)$ in the disk plane at different moments: a) $t = 2.7$ – the mode $m = 2$ develops itself in the central region, b) $t = 3.1$ – $m = 2 \rightarrow m = 1$ reorganization, c) $t = 4.2$ – a well-developed one-arm mode $m = 1$, d) $t = 10.1$ – $m = 1 \rightarrow m = 0$ reorganization, e) $t = 16.4$ – a well-developed symmetric mode $m = 0$, g) $t = 51$ – all perturbations in the center $r \lesssim L = 0.25$ have almost gone out. In the middle regions one can see the axisymmetric perturbations and the mode $m = 2$ takes place at the outer parts of the disk.

bulge and as a correct approach a non-stationary model for the bulge has to be evaluated, hence this our result require further investigation. Meanwhile we constrain our study in § 4 by the case of galaxies without large bulges.

The bending modes $m = 1, 2$. In the models with a massive halo ($\mu \gtrsim 2$) the axisymmetric bending modes $m = 1$ and $m = 2$ may develop themselves and heat up the disk in the vertical direction. The surface density of the disk remains axisymmetric. The evolution of initially thin disk for $\mu = 4$ is shown in Fig.1 g-i. In the latter case the bending mode $m = 2$ of saddle-type is being developed firstly in central disk regions ($r \lesssim 2L$). Fig.4 shows the distribution of ζ in the disk plane for different moments of $t = 0 \div 40$. The vertical heating and disk’s flare due to the mode $m = 2$ is very modest in this case. However, after $t \gtrsim 3$ the non-linear stage of one-arm asymmetric mode $m = 1$ develops itself and the vertical heating gets more significant. The third stage of the heating begins at $t \gtrsim 10$ when the mode $m = 0$ begins to dominate in the disk. The growth rate of the vertical dispersion c_z is especially high at this time; the disk scale height increases by a factor of 2 – 3. The example considered shows the process of transformation between the bending modes and transition

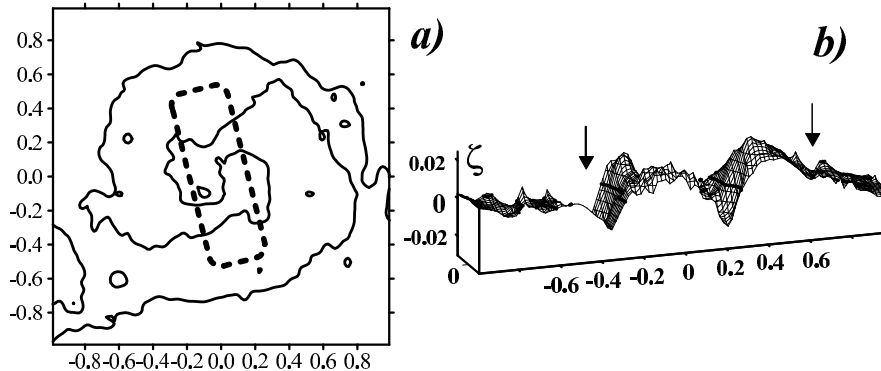


Fig. 5.— a) The distribution of ζ in the disk plane (dash-line shows the bar position, the solid line marks $\zeta = 0$). b) The vertical profile of ζ taken along the bar. The arrows mark the bar edges).

from the asymmetric mode $m = 2$ to the axisymmetric one.

As well as for the case of the spherical subsystem of low mass, the favourable conditions for the emerging of the global bending instability get worse and, starting with some $\alpha_z(r)$, the disk warp does not develop itself for at least 20 rotation turns if the initial $\alpha_z = c_z/c_r$ (and $z_0(r)$ respectively) is high enough.

A stellar disk developing the bending instability with $m = 1, 2$ is not in a quasi steady-state in the vertical direction. The distribution of c_z remains axisymmetric, in a contrary to z_0 . Hence, the condition $c_z^2/z_0 = const$ is failed and this instability evolves rapidly. For the axisymmetric mode the condition $c_z^2 \propto z_0$ is fulfilled much better except the very central region of the disk in stages when the thickness rises significantly.

Apparently, an essential part of real stellar disks did not undergo the heating due to the axisymmetric bending mode $m = 0$ because this mode would produce too thick disks. As an example, in the experiment shown in Fig.1 ($\mu = 1$) the disk scales ratio $\langle z_0 \rangle / L \simeq 0.4$ (here $\langle z_0 \rangle$ denotes the average thickness over the disk). The relation c_z/c_r exceeds its critical value for the final state of disk. The relative thickness is less ($\langle z_0 \rangle / L \simeq 0.16$) for the case of massive halo ($\mu = 4$) after the relaxation of the axisymmetric mode. On the other hand, there are galaxies which have the ratio $\langle z_0 \rangle / L \leq 0.15$. According to our assumptions either the very massive halos are required for this case, or the axisymmetric bending mode $m = 0$ was never developed in those galactic disks.

Bendings of bar. Let's consider the experiments with rather light halo ($\mu \lesssim 1.5$). If the initial state of disk is gravitationally unstable, a bar can be developed. The bar formation is accompanied by its warps (Raha et al. 1991). The bendings of a bar can emerge as a result

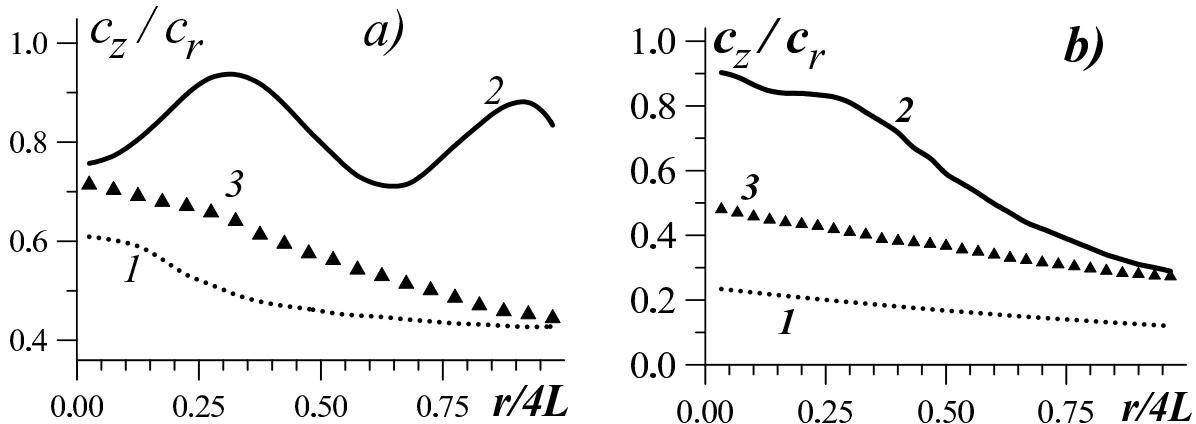


Fig. 6.— The radial distribution of $\alpha_z = c_z/c_r$ for: a) $\mu = 1$ (see Fig.1a-f), b) $\mu = 4$ (see Fig.1g-i). 1 – the initial distribution, 2 – the final distribution, and 3 – the critical level of α_z .

of global instability of the bar-mode during its initial stage when the bar forms in initially thin cold disk. Fig.5 shows the bar bending which increases the vertical velocity dispersion with time. The amplitude of the bar warps falls essentially with increasing the bar thickness. Let’s stress that once the bar has been formed, it stops the further possible developing of the global bending modes, thus it destroys the axisymmetric mode $m = 0$ first of all.

The bar formation occurs faster in the case of cold initial disk (for small values of the Toomre stability parameter Q_T) and as a result, the bar bending amplitude rises (Fig.5). If the initial disk was in a marginally subcritical state (i.e. c_r was just below the critical value which provides stability against the global bar-mode), the bar forms very slowly and it is stable against the bending perturbations.

The ratio c_z/c_r . With the similar values of parameters in our model, the key parameter responsible for the stellar disks stability is the ratio $\alpha_z = c_z/c_r$. To stabilize the global bending perturbations in the case of low relative mass of the spherical subsystem, the values of c_z/c_r have to be larger than 0.3 – 0.37 what was figured out from linear analysis in simple models (Poliachenko & Shuhman 1977; Araki 1986; Merrit & Sellwood 1994). Let’s consider bulgeless model with a moderate halo $\mu = 1$ (see Fig.6). The initial (curve 1) and final (curve 2) distributions of $\alpha_z(r)$ are shown in Fig.6a. The vertical heating of disk originated from the axisymmetric bending mode development is as strong that the averaged throughout the disk ratio $\langle c_z/c_r \rangle = 0.82$. If the initial ratio $\alpha_z(r)$ follows the curve 3, then the global bending modes stay stable.

Once the relative mass of halo rises gradually, the ratio c_z/c_r needed to marginally

stabilize the bending perturbations (we will denote it as the critical α_z ratio) is getting less. The initial (curve 1) and final (curve 2) distributions of $\alpha_z(r)$ for the case of very massive halo of $\mu = 4$ are shown in Fig.6b. The curve 3 shows the initial distribution of $\alpha_z(r)$ needed to provide the stability against the global bending modes. At the same time in the disk periphery $0.27 < c_z/c_r < 0.37$.

A distinctive feature of the considered models at the threshold of bending stability is the non-uniformity of c_z/c_r along the radius (see Fig.6). For the case of moderate halo ($\mu \lesssim 1$) and when the initial distribution of $c_r(r)$ suppresses the bar instability, the critical value of α_z^{crit} is a declining monotonous function of r : its typical values range from $0.7 \div 0.8$ at the central regions to $0.4 \div 0.5$ at the periphery.

In both cases of large and small μ , the ratio of velocity dispersions c_z/c_r falls exponentially with radius and can be approximated as $\alpha_z^{crit} \propto \exp(-r/L_\alpha)$ with scale $L_\alpha \simeq (4-6) \cdot L$.

There are two reasons of decreasing the disk thickness with the rising of the halo mass. At first, the ratio c_z/c_r needed to stabilize the bending instability is lower. On the other hand, the halo suppresses the gravitational instability in the plane of disk, therefore c_r/V falls (Khoperskov et al. 2001; Khoperskov et al. 2003). Note that in real galaxies several more factors such as density waves, scattering on giant molecular clouds, and tidal interactions heat up the disk and increase its scale height. Then α_z^{crit} and the corresponding disk thickness gives us the lower estimate for the halo mass.

4. The results of dynamical modeling of edge-on galaxies

In order to compare our model predictions with observations, we consider seven spiral edge-on galaxies. Four of them, NGC 4738, UGC 6080, UGC 9442, and UGC 9556 have no bulges and their structural parameters were derived by (Bizyaev & Kajsin 2002). The radial distribution of their stellar disks' thickness is available. The galaxy UGC 7321 is interesting for us because of its superthin disk and low surface brightness nature (Matthews 2000). For two large and nearby galaxies, NGC 891 and NGC 5170, the data on the radial component of stellar velocity dispersion are available from published data (Bottema et al. 1987; van der Kruit & Searle 1981; Bahcall & Kylafis 1985; Shaw & Gilmore 1989; Morrison et al. 1997; Xilouris et al. 1999; Sancisi & Allen 1979; Begeman et al. 1991; Bottema et al. 1991). It enables us to incorporate those data together with the structural parameters of disks. The name of galaxy, the adopted distance D , the radial scale length L , the averaged scale heights $\langle z_0 \rangle$ and $\langle h_z \rangle$ (corresponding to *sech*² and *exp* distributions in the vertical direction respectively), and the stellar disk maximum radius R_{max} are shown in Table 1.

Table 1: Parameters of the edge-on galaxies

Name	D Mpc	L kpc	$\langle z_0 \rangle$ kpc	$\langle h_z \rangle$ kpc	R_{max} kpc	μ
UGC 6080	32.3	2.9	0.69	0.48	9.9	0.57
NGC 4738	63.6	4.7	1.3	0.7	19.2	0.7
UGC 9556	30.6	1.5 (3.6)	0.51	—	9	1.1
UGC 9422	45.6	3.5	0.80	0.51	14.6	0.8
NGC 5170	20	6.8	0.82	—	26.2	1.38
UGC 7321	10	2.1	0.17 ^a	0.14 ^b	8.2	2.3
NGC 891	9.5	4.9	0.98	0.49	21	0.89

^a the scale is shown for the disk’s periphery in the case of $sech(z/z_{ch})$.

^b the scale is shown for the disk’s central region.

Here D is the distance to the galaxy ($H_0 = 75 \text{ km s}^{-1} \text{ Mpc}^{-1}$), L is the exponential disk scale length, $\langle z_0 \rangle$ is the averaged over the disk value of the vertical scale height for $sech^2$ vertical profile, $\langle h_z \rangle$ is the scale height averaged over the disk for the exponential vertical profile, R_{max} is the maximum radius of the stellar disk.

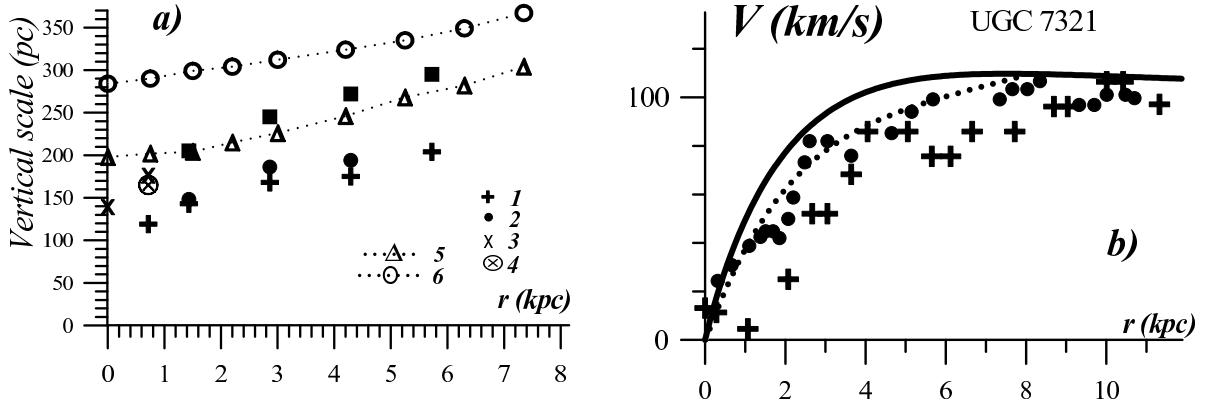


Fig. 7.— a) The radial distribution of the scale height in UGC 7321. The observational data: 1 and 2 – for the case of $sech(z/h_{ch})$ density distribution in the vertical direction, 3 and 4 — for the exponential law $\exp(z/h_z)$. b) The rotation curve of UGC 7321. The symbols + and • represent the observational data for both sides from the center.

As an example, we consider the modeling of UGC 7321. The galaxy UGC 7321 reveals itself as a superthin (Goad & Roberts 1981) and bulgeless (Matthews et al. 1999) disk galaxy. The disk thickness was derived by (Matthews 2000). We choose the systematic radial velocity of 394 km/s as that the maximum rotational velocity at the periphery has the similar values ($V \simeq 100 \text{ km/s}$) in both sides of the galaxy. The curves 5 and 6 in Fig.14 are

calculated for the models with $\mu = 2.3$ and 1.5 , respectively, inside of $r = R_{max}$. As it is seen, the model with $\mu > 3$ gives a better agreement with the observed radial distribution of the vertical thickness. The best fit model with $\mu = 2.3$ has $M_d = 0.62 \cdot 10^{10} M_\odot$ and $M_h = 1.4 \cdot 10^{10} M_\odot$.

The evaluated best-fit parameters μ (spherical-to-disk mass ratios) are shown in Table 1. Since five of our galaxies have no bulges, and the bulges of another two are relatively small, the values of μ represent the relative dark halo masses. As it can be seen from the Table 1, the dark and luminous matter contributions are comparable inside the stellar disk limits in our galaxies. The exception is the superthin galaxy, UGC 7321, which has a massive dark halo and a low surface brightness disk.

5. Conclusions

1. The development of the bending instabilities in stellar galactic disks is studied with the help of N-body numerical simulations. The axisymmetric bending mode ($m = 0$) is found to be the strongest factor which may heat up stellar disks in the vertical direction. If a bar formation was suppressed, the role of ($m = 1$) and ($m = 2$) bending modes in the disk thickening would be low. The most significant thickening of the stellar disk occurs at the initial non-linear stage of the bendings formation. Once the bendings are destroyed, the vertical heating becomes less effective. The lifetime for the bending mode $m = 0$ increases with the growth of the relative mass of the spherical subsystem μ . We show that the initially thin disks increase their thickness much more rapidly than those started from a marginally subcritical state. It is important to notice that the final disk thickness and c_z depend on its initial state and the definition of stability boundary requires a special approach.
2. The critical values of the ratio $\alpha_z^{crit} = c_z/c_r$ are considered as a function of the spherical subsystem parameters. At the threshold of stability, the value of $\alpha_z^{crit}(r)$ falls with the distance to the center. The value of α_z^{crit} can be twice less at the periphery in comparison with its central value.
3. The averaged relative disk scale height $\langle z_0 \rangle / L$ falls when the relative halo mass increases. We use this kind of relation to estimate the mass of the spherical subsystem for edge-on galaxies.
4. We conduct N-body modeling for seven edge-on galaxies based on published rotation curves and surface photometry data (for two galaxies we incorporate the data on the observed stellar radial velocity dispersion in addition). The relative mass of the spherical subsystem (dark halo in most cases) is inferred for all the galaxies. The evaluated mass of the dark halo

in our galaxies is of order of their disk’s mass. As an exception, the superthin LSB galaxy UGC 7321 own the dark halo which contains more than 2/3 of overall galaxy mass.

This work is supported by the Russian Foundation for Basic Research through the grants RFBR 04-02-16518, 04-02-96500 and by the Technology Program “Research and Development in Priority Fields of Science and Technology” (contract 40.022.1.1.1101).

REFERENCES

- Araki, S. PhD Thesis 1986, Massachusetts Institute of Technology
- Athanasoula, E., Sellwood, J.A. 1986, MNRAS, 221, 213
- Bahcall, J. 1984, ApJ, 276, 156
- Bahcall, J.N., Kyllafis N.D. 1985, ApJ, 288, 252
- Bailin, J., Steinmetz, M. 2003, Ap.&Space Sci., 284, 701
- Binney J., Jiang, I.-G., Dutta, S. 1998, MNRAS, 297, 1237
- Bizyaev, D., Kajsin, S. 2002, AAS, 201, 46.05
- Bottema, R., Gerritsen, J. 1997, MNRAS, 290, 585
- Bottema, R., van der Kruit, P., Freeman, 1987, A&A, 178, 77
- Bottema, R., van der Kruit, P.C., Valentijn, E.A. 1991, A&A, 247, 357
- Begeman, K.G., Broeils, A.H., Sanders, R.H. 1991, MNRAS, 249, 523
- Carlberg R.G., Sellwood J.A. 1985, ApJ, 292, 79
- Fuchs, B., von Linden S. 1998, MNRAS, 294, 513
- Goad, J., Roberts, M. 1981, ApJ, 250, 79
- Griv, E., Yuan, C., Gedalin, M. 2002, ApJ, 2002, 580, 27L
- Hernquist, L., Heyl, J., Spergel, D. 1993, ApJL, 416, 9
- Holley-Bockelmann, J., Mihos, J., 2001, AAS, 198, 08.15
- Khoperskov, A., Zasov, A., Tyurina, N. 2001, Astron.Rep., 45, 180

- Khoperskov, A., Zasov, A., Tyurina, N. 2003, *Astron.Rep.*, 47, 357
- Mayer, L., Governato, F., Colpi, M., et al. 2001, *ApJ*, 559, 754
- Matthews L.D., Gallagher J.S., van Driel W. 1999, *AJ*, 118, 2751
- Matthews, L.D. 2000, *AJ*, 120, 1764
- Merritt, D., Sellwood, J. 1994, *ApJ*, 425, 551
- Mikhailova, E., Khoperskov, A., Sharpak, S. 2001, in "Stellar dynamics: from classic to modern", ed. L.P. Ossipkov, I.I. Nikiforov, (Saint Petersburg), 147
- Morrison, H., Miller, E., Harding, P., Stinebring, D., et al. 1997, *AJ*, 113, 2061
- Ostriker, J., Peebles, P. 1973, *ApJ*, 186, 467
- Patsis P.A., Athanassoula E., Grosbol P., Skokos Ch. 2002, *MNRAS*, 335, 1049
- Pohlen, M., Dettmar, R.-J., Lutticke, R., Aronica, G. 2002, *A&A*, 392, 807
- Poliachenko, V., Shuhman, I. 1977, *Sov.Astron.Lett.*, 3, 134
- Poliachenko, V.L., Shukhman, I.G. 1979, *Sov. Astr. Rep.*, 23, 407
- Raha, N., Sellwood, J., James, R., Kahn F. 1991, *Nature*, 352, 411
- Reshetnikov, V., Combes, F. 2002, *A&A*, 382, 513
- Sancisi, R., Allen, R.J. 1979, *A&A*, 74, 73
- Sellwood, J. 1996, *ApJ*, 473, 733
- Sellwood J.A., Merritt D. 1994, *ApJ*, 425, 530
- Shaw, M.A., Gilmore, G. 1989, *MNRAS*, 237, 903
- Sotnikova, N., Rodionov, S. 2003, *Astronomy Letters*, 29, 321
- Toomre, A. 1966, *Geophys. Fluid Dyn.*, No. 66–46, 111
- Valluri M. 1994, *ApJ*, 430, 101
- van der Kruit, P., Searle, L., 1981, *A&A*, 95, 116
- van der Kruit, P., Searle 1982, *A&A*, 110, 61

Vandervoort, P. 1991, ApJ, 377, 49

Velazquez, H., White, S. 1999, MNRAS, 304, 254

Weinberg, M. 1998, MNRAS, 299, 499

Xilouris, E.M., Byun, Y.I., Kyllafis, N.D., et. al. 1999, A&A, 344, 868

Zasov, A., Makarov, D., Mikhajlova, E. 1991, Sov.Astron.Lett., 17, 374

Zasov, A.V., Khoperskov, A.V. 2003, Astron. Letters, 29, 437

